Chapter 3: Analysis of reported case histories of pile foundation performance during earthquakes

3.1 Introduction

A significant number of cases of performance of pile-supported structures during earthquake liquefaction have been reported in the literature. Some pile foundations were found to survive earthquakes while others suffered severe damage. Fifteen cases of pile foundation performance are analysed and presented in this chapter, giving emphasis to the slenderness of the piles. The study of the case histories seems to show dependence of pile performance on certain parameters and also an insight to the modes of failure. A thorough analysis of these parameters is carried out to formulate a hypothesis of pile failure based on buckling. This hypothesis is later verified using dynamic centrifuge modelling as discussed in chapters 4 and 5.

This chapter is divided into three sections. In the first section (3.2), a methodology of analysis of case histories is formulated. The assumptions in the methodology are also stated. The second section (3.3 & 3.4) describes the case histories and presents their analysis. The results of the analysis are summarised in the forms of plots and tables. In the third section (3.5) a hypothesis of pile failure is postulated.

3.1.1 Past work and this study

There has been a large volume of material published on observations of pile damage during past earthquakes (see for example, (Mizuno, 1987), (Youd, 1993), (Hamada, 1992a, 1992b), (Tokimatsu et al. 1997,1998,1999), (Ishihara, 1993,1997), (Yokohama et al., 1997)). They mainly consist of a reconnaissance survey after an earthquake. A summary of the above reports can be found in Dobry and Abdoun (2001). Mizuno (1987) compiled thirty cases of pile damage during earthquakes in Japan for a period of 60 years between 1923 and 1983. This paper lists the earthquakes, damage of superstructure, types of piles and in some cases the dimensions of the piles. Berrill et al. (2001) documented in detail the good performance of the Landing Bridge during the 1987 Edgecumbe earthquake. All the above studies assumed the pile as being a beam element. Most of the conclusions are qualitative and are in favour of bending failure.

In contrast, the analysis of case histories presented in this thesis assumes the pile as being a column element. Also an attempt has been made to quantify some parameters such as the superstructure load acting on the pile during earthquake. In short, emphasis is given to the structural nature of the pile.

3.2 Method of analysis of case histories

The main assumptions in the analysis of the case histories are:

1. Piles are slender columns having support from the surrounding soil. During earthquake liquefaction, soil does not offer sufficient support and the pile acts as an unsupported column.
2. A piled structure such as a bridge or building is considered as a frame supported on slender columns. Each of these structures has a critical load i.e. the minimum axial load at which the frame would become unstable. Lateral load or perturbations would decrease the critical load. Example for buckling of frames having slender columns of Length (L) to Diameter (D) ratio of 93 is shown in Figures 3.1 and 3.2. Figure 3.1 may represent a row of piles in the absence of soil as in the Showa Bridge, Figure 1.2b, 1.7, and 1.8. On the other hand Figure 3.2 may represent a piled raft or a pile group in the absence of soil. It must be remembered that piles normally have (L/D) ratio of 25 to 100 (see Figure 2.9).

3. The design axial load on each pile from the superstructure under the worst credible loading condition will be equal to the allowable load in the pile predicted by the soil properties. This assumption can make a reasonable estimation of the axial load acting on the pile during earthquake.

The third assumption is demonstrated in section 3.2.1, using the example of the Showa Bridge.

Figure 3.1: A row of slender columns representing a row of piles.

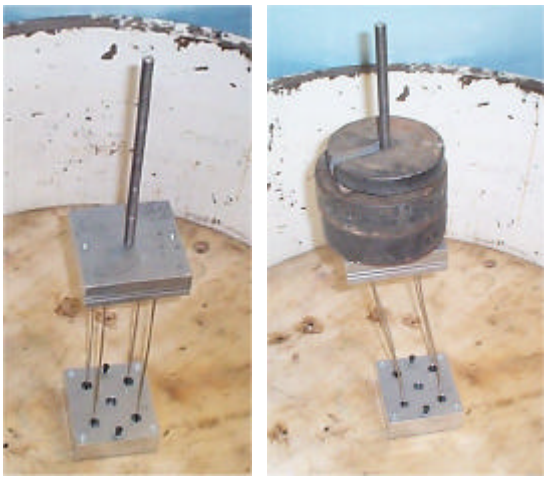

Figure 3.2: A group of slender columns representing a pile group.

3.2.1 Example of the Showa Bridge

The example is the collapse of the Showa Bridge over river Shinano in Japan during the 1964 Niigata earthquake. The bridge failed only one month of its completion. The failure of the bridge as shown in Figure 1.2(b), 1.7 and 1.8 is well documented by Iwasaki (1984) and Fukuoka (1966). Iwasaki (1984) describes the superstructure and the type of bridge. Fukuoka (1966) reports the soil profile after the earthquake. In this section the axial load acting on the structure will be back calculated based on the two approaches.

1. PILE CAPACITY APPROACH

The pile capacity is estimated based on SPT values quoted in Figure 3.3(a) (Figure 2.16 reproduced here). Standard correlations, Randolph (1985) have been used and the values are shown in Figure 3.3(b) (see Table 2.4 for pile parameters).

Shaft resistance

Layer 1 (outer) = $\pi \times 0.609\text{m} \times 10\text{m} \times 30\text{kPa} = 573$ kN

Layer 2 (outer) = $\pi \times 0.609\text{m} \times 6\text{m} \times 50\text{kPa} = 573$ kN

Base resistance

Plugged mechanism = $\pi/4 \times (0.609)^2\text{m}^2 \times 7500\text{kPa} = 2184$ kN

Unplugged mechanism = $\pi/4 \times [(0.609)^2 - (0.591)^2]\text{m}^2 \times 7500\text{kPa} = 127$ kN

ULTIMATE PILE CAPACITY

Plugged mechanism = (573 + 573 + 2184) kN = 3300 kN

Unplugged mechanism = $[(573 + 573) \times 2 + 127]$ kN = 2419 kN

ALLOWABLE LOAD IN PILE (using a factor of safety of 2.5)= 2419 / 2.5 = 965 kN

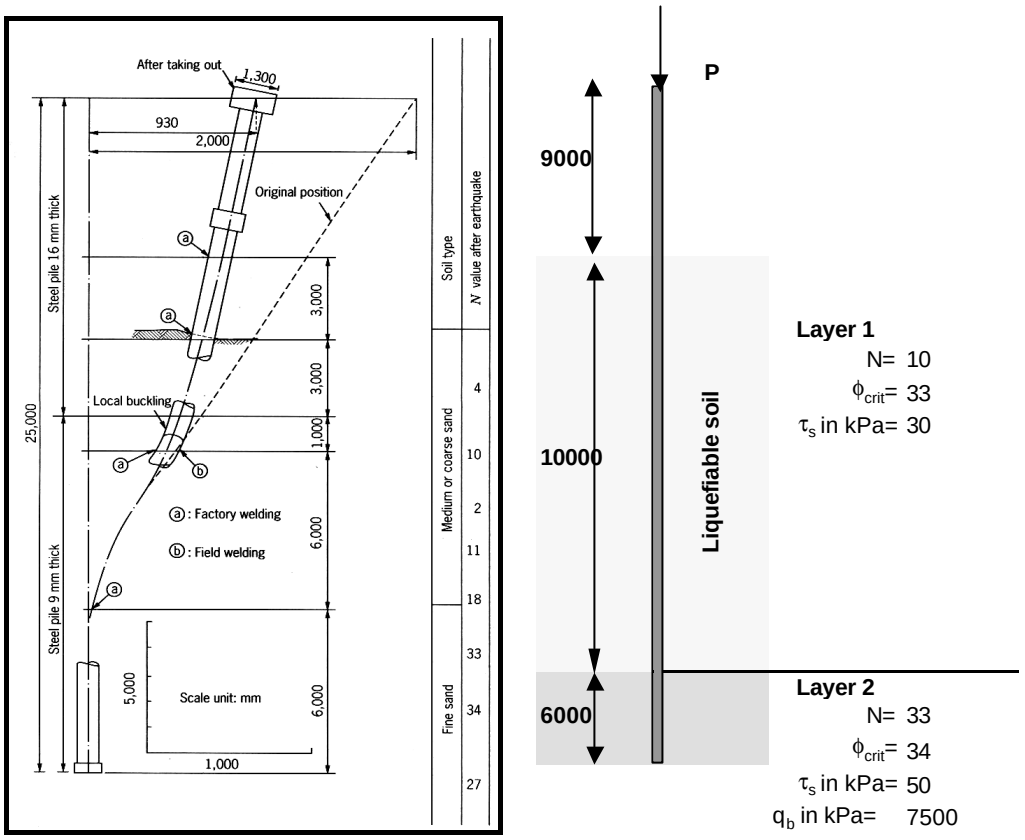

Figure 3.3: Piles of Showa Bridge; (a): Post earthquake recovery (Figure 2.16 reproduced) after Fukoka (1966); (b): Schematic diagram of the pile and the soil profile.

2. SUPERSTRUCTURE LOAD APPROACH

This section calculates the dead load on each pile from the configuration of the Showa Bridge deck (see Figure 3.4). Information of the dimensions of the girders, span and the bridge type is obtained from Iwasaki (1984). Reasonable assumptions are made for the missing data. A schematic diagram of the deck is shown in Figure 3.5.

The bridge has a total length of 303.9 m (13.75 m + 10@ 27.64 m + 13.75 m) and width of 24 m. The superstructure of the bridge consists of 12 composite steel simple span girders. There are 9 piles in a row sharing the load of the superstructure (see Figure 1.7). Table 3.1 shows the estimate of the total dead load for each span. It is assumed in the analysis that the load of the deck is shared equally by each of the piles.

It is very interesting to note that the dead load per pile is in the order of 740 kN. If the live load due to the vehicular loading is added, the total load will be near 1000 kN. The allowable load predicted based on the soil parameter (N values) is 965kN.

Table 3.1: Dead load calculation for Showa Bridge

Item	**Details**	**Load**
Slab and asphalt top	$24.8m \times 27.64m \times (0.2+0.05)m \times 25kN/m^3$	4146kN
Crash barrier	$2 \times 1.5m \times 0.1m \times 27.64 \times 25kN/m^3$	207.3kN
Kerb	$2m \times 0.15m \times 27.64m \times 25kN/m^3$	207kN
9 steel girders	$27.64m \times 9 \times 5.2kN/m$	1294kN
Stiffeners, bolts	30% of girder weight	388kN
Bottom Girder	$0.7m \times 1.0m \times 24m \times 25kN/m^3$	420kN
Total		6662kN
Load per pile = 6662kN/9		**740kN**

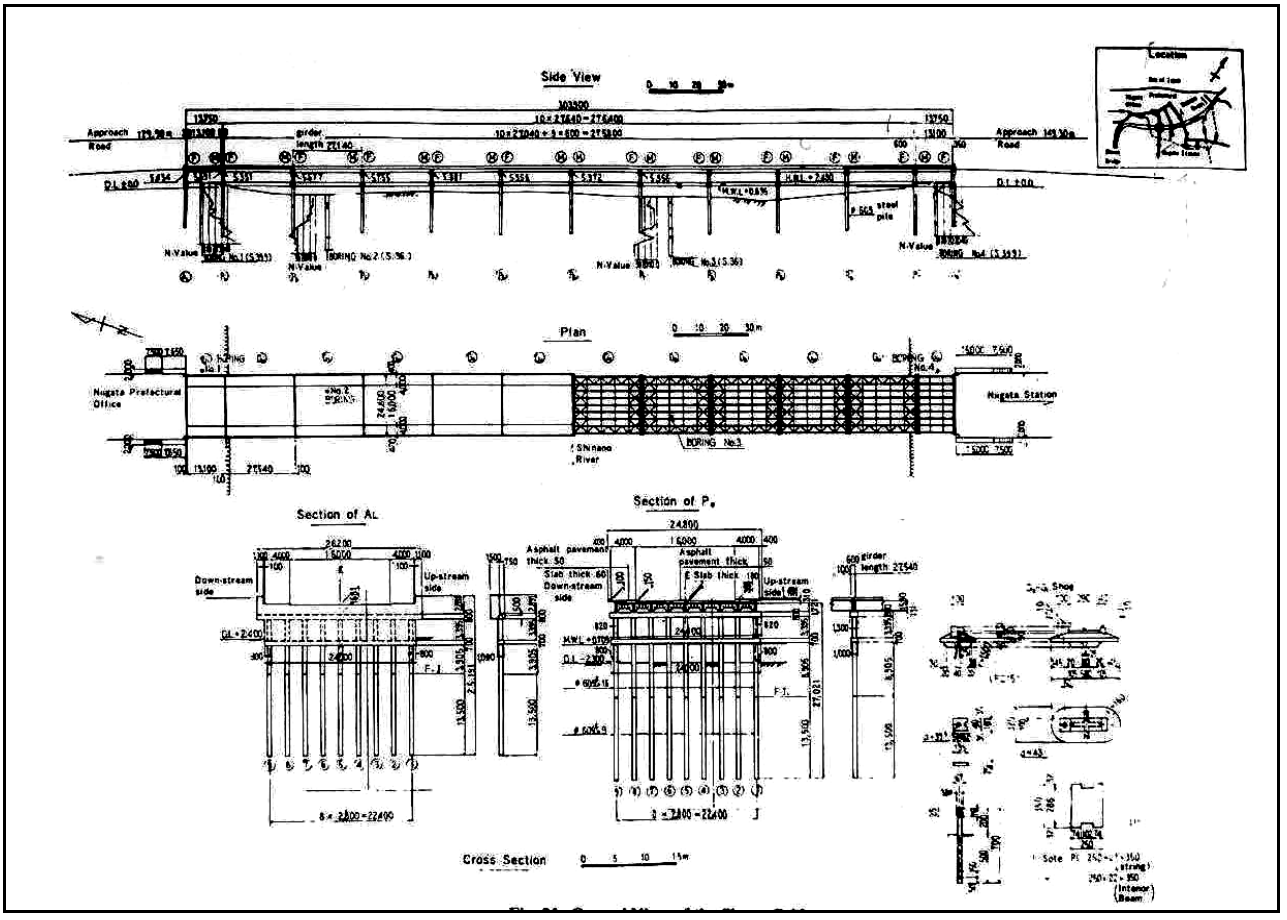

Figure 3.4: Structural details of the Showa Bridge deck, Iwasaki (1984). The relevant part of the superstructure necessary for calculations is redrawn in Figure 3.5

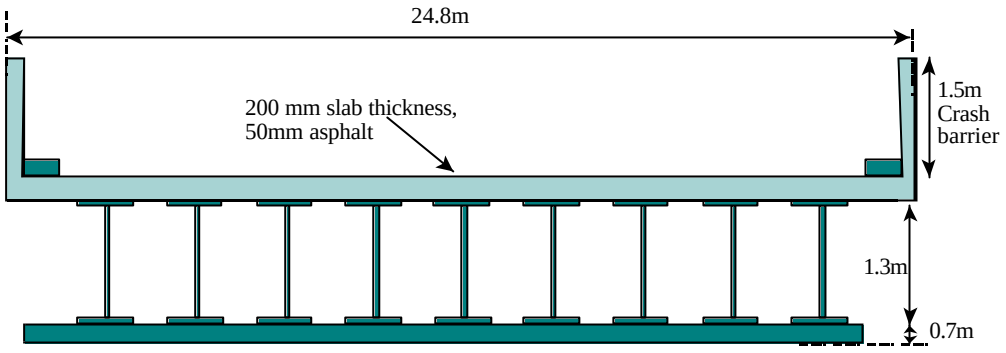

Figure 3.5: Schematic of the Showa Bridge deck

It is worth mentioning that for NFCH building (described in the next section) the allowable estimated based on the conventional pile capacity method is 287 kN whereas the actual load applied is 292 kN as reported by O'Rourke et al (1994).

3.2.2 Parameters in the analysis

As mentioned earlier, the case histories are analysed giving emphasis to buckling characteristics. The parameters in the analysis are:

- L_{eff}= Effective length of the pile in the liquefiable region. The definition of effective length shown in Figures 3.6 and 3.7 has been adopted from column stability theory and is chosen to normalise the different boundary conditions of pile tip and pile head. Figure 3.6 links to the failure observed in Figure 3.2. L_{eff} is also familiar as the "Euler's buckling length" of a strut pinned at both the ends. In practice, designers may prefer to extend the effective length by a few diameters to account for imperfect fixity in the non-liquefying layer (see for example Fleming et al., 1992).
- r_{min} = minimum radius of gyration of the pile given by equation 2.1.
- Slenderness ratio of the pile in liquefiable region, L_{eff}/r_{min}.
- Allowable load on the pile, P, based on conventional design procedures, with no allowance for liquefaction. This can also be called as conventionally allowable load in the

pile. This is calculated based on Class A prediction using the available soil parameters provided by the author of the case history.

- Euler's elastic critical load of the pile (P_{cr}) calculated from the well-known buckling formula as shown by equation 3.1.

$$P_{cr} = \frac{p^2}{L_{eff}^2} EI \qquad (3.1)$$

- Axial stress σ in the pile, calculated by dividing P by the cross-sectional area of the pile, A. The value at failure is denoted as σ_f.

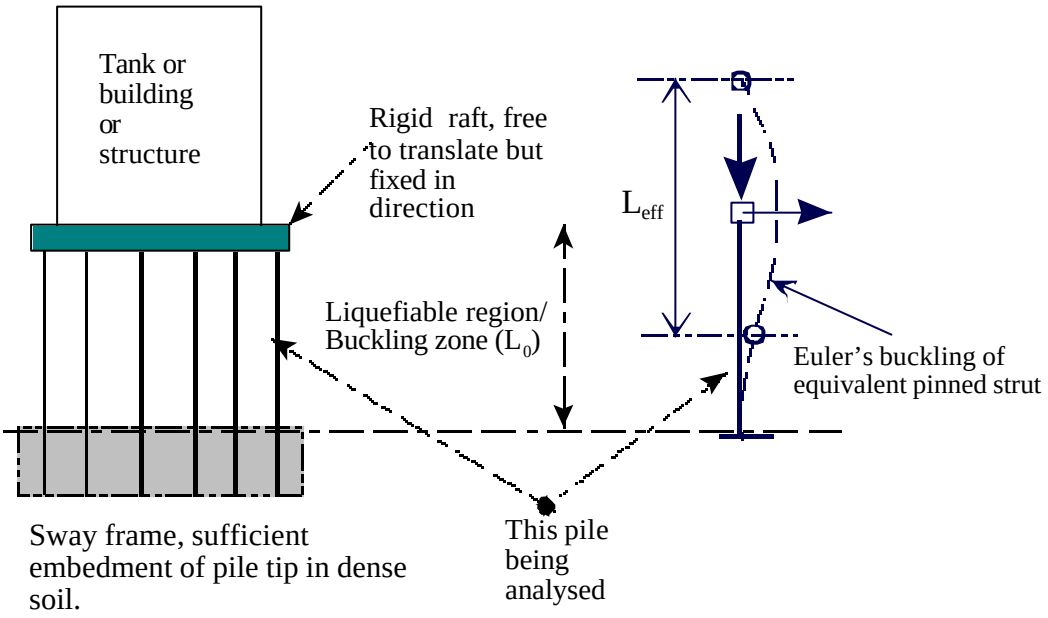

Figure 3.6: Effective length for a tank type structure

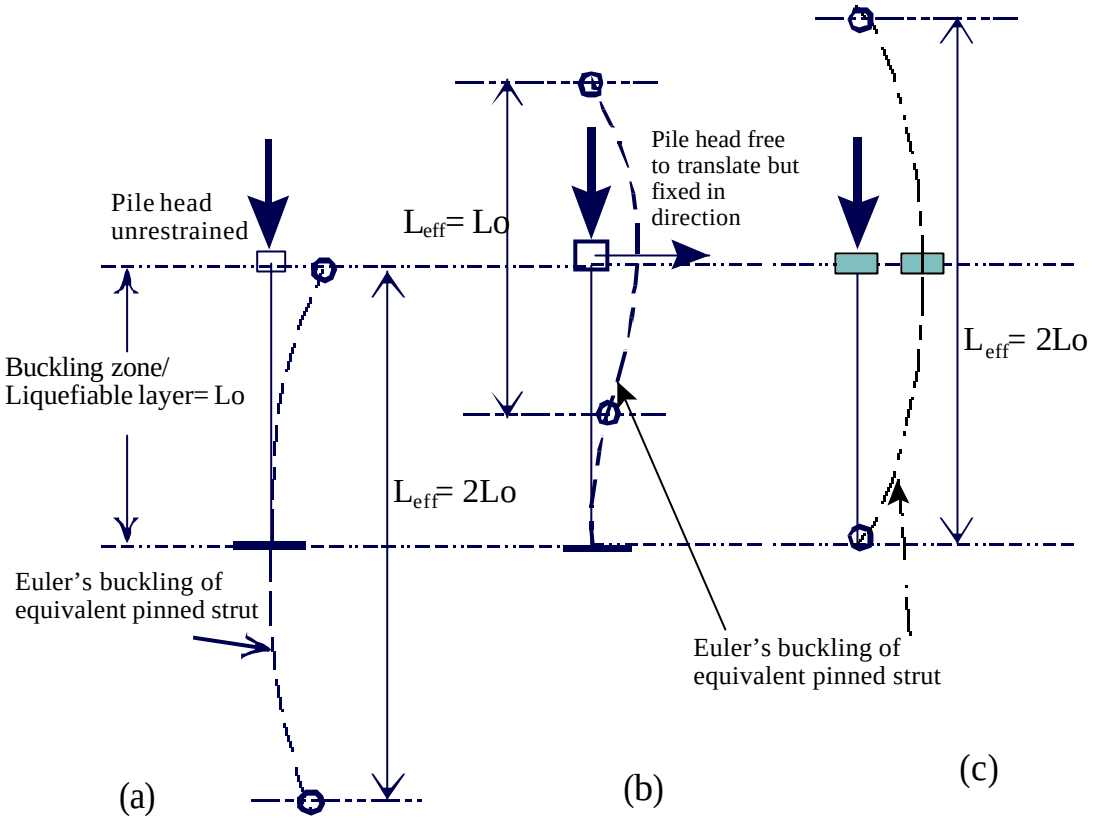

Figure 3.7: Concept of effective length of pile for different boundary conditions.

3.3 Reported case histories of pile foundation performance during earthquakes.

This section of the chapter describes the fifteen case histories studied and analysed. Out of the fifteen case histories, six were found to survive the earthquake and the remaining nine either collapsed or suffered severe damage. This section is divided into two subsections. In the first subsection the structures that performed well are described and in the second subsection, the structures that performed poorly are presented. Detailed calculations are omitted in the interests of brevity. Representative sample calculations for two case histories (one good performance and one poor performance) are shown in Appendix C. The parameters mentioned in section 3.2.2 for each of the fifteen case histories are tabulated in Table 3.4.

3.3.1 Good performances of pile foundations

Table 3.2 lists the case histories described in this section along with the reference to the author. As mentioned earlier, Table 3.4 summarises the parameters of the analysis.

Table-3.2: Good performance of pile foundations.

Index no	Earthquake	Structure type	Reference
1	1964 Niigata earthquake, Japan	10-storey piled raft with basement building in a laterally spreading soil.	Hamada (1992a)
2	1987 Edgecumbe earthquake, New Zealand	Landing bridge in a laterally spreading soil	Berrill et al. (2001)
3	1995 Kobe earthquake	14 storey building in American Park	Tokimatsu et al. (1996)
4	1995 Kobe earthquake	Kobe Shimim hospital	Soga (1997)
5	1995 Kobe earthquake	Hanshin Expressway pier-211	Ishihara (1997)
6	1995 Kobe earthquake	LPG tank 101	Ishihara (1997)

Case history 1

10-storey Hokuriku building during the 1964 Niigata earthquake

The first case study shows the good performance of a 10-storey building, which has a basement floor and founded on reinforced concrete piles. The piles have a diameter of 400mm and a length of 12 m. No damage was reported to the superstructure after the earthquake. It was also reported that no cracks formed on the walls, beams, and columns and furthermore, that no inclination occurred. The ground surface nearby the building moved by about 2 m (see Hamada, 1992a). Thus the building performed well in spite of severe lateral spreading. A schematic diagram of the building and the soil profile are shown in Figure 3.8.

The pile passed through a maximum of 5 m in liquefied soil layer and is embedded 7m in dense soil (see Hamada, 1992a). The pile top is integrally cast with the basement slab. The pile tip can be assumed to be fixed at the dense sand layer while the top head can be assumed free to translate laterally but held in direction as shown in Figure 3.6. The parameters are listed in Table 3.4. Appendix C shows in detail derivation of these parameters.

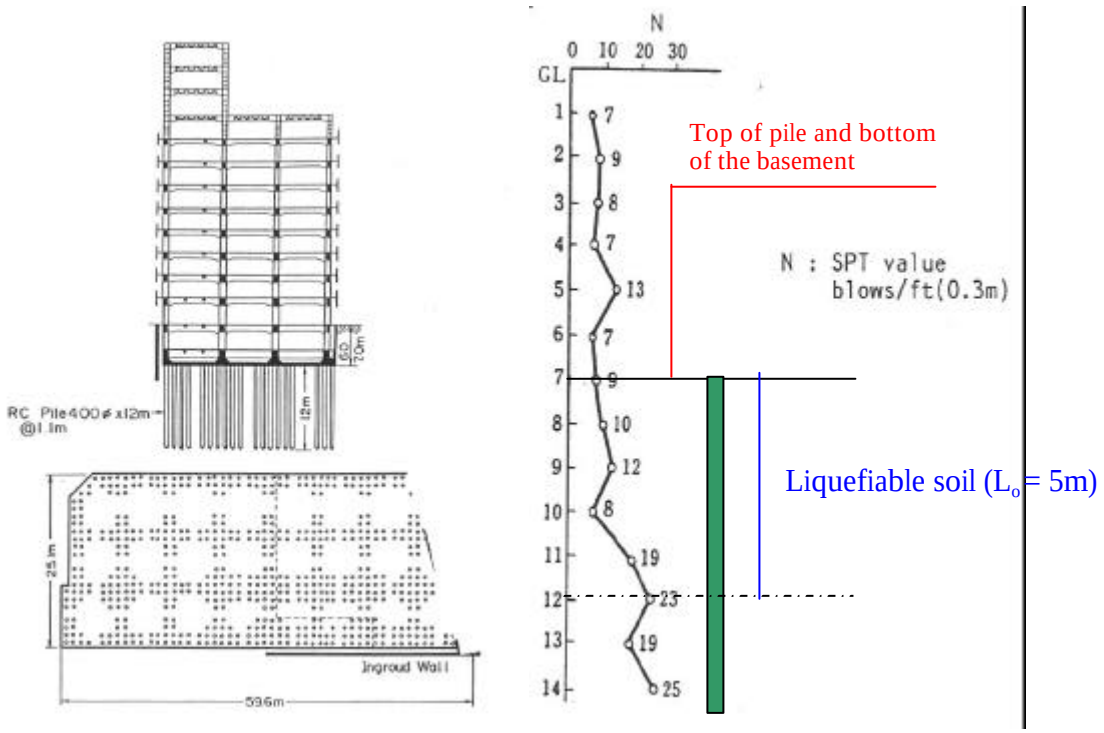

Figure 3.8: The structural arrangement of the 10-storied piled building along with the soil profile (after Hamada, 1992a).

Case history 2

Landing Bridge during the Edgecumbe Earthquake of March 2, 1987

The second case study illustrates the good performance of Landing Road Bridge (Whakatane, New Zealand) in spite of extensive lateral spreading around the bridge. The bridge was constructed in 1962, and comprised 13 simply supported spans 18.3 m long carrying a two-lane, cast-in-place concrete deck and two foot-paths (see Figure 3.9). Details of the post-earthquake study can be seen in Berrill et al. (2001). The water table is at about 1.5 to 2 m below ground level, depending on the level of the tidal river. The logs show that the piles passed through 1-2 m in clayey silt (non-liquefiable), then through 4m in liquefiable deposit and finally driven into 2-3 m into dense sand. The piles are 406 mm square pre-stressed concrete piles at 1:6 rake. The field investigating team reports that there was clear evidence of liquefaction and passive failure of the non-liquefiable crust, which drove against the piles.

The foundation capacity against lateral loads is estimated based on the collapse mechanism shown in Figure 3.10(a). Detailed estimation of collapse load of the structural system can be seen in Berrill et al. (2001). The result is shown in Figure 3.10(b).

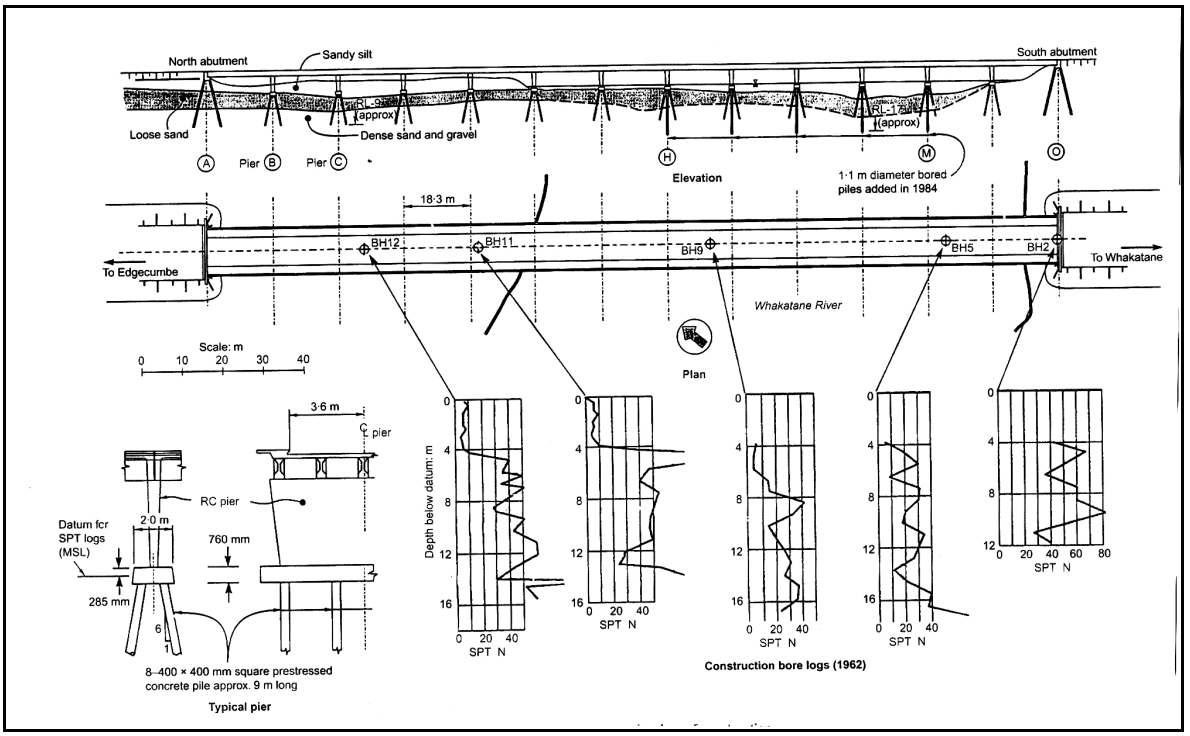

Figure 3.9: Plan and structural details of the Landing Road Bridge that sustained the 6.3 earthquake in spite of lateral spreading (after Berrill et al., 2001).

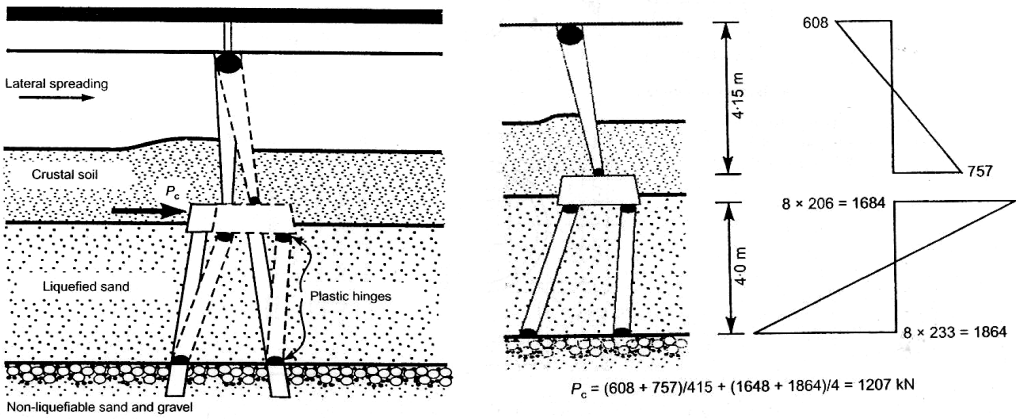

Figure 3.10: (a): Assumed substructure collapse mechanism to predict the capacity of the foundation (after Berrill et al. 2001); (b): Collapse load for the pier system calculated from plastic moment (after Berrill et al., 2001).

In the Figure 3.10(b) plastic moments at the top of the pier, bottom of the pier, pile at pile cap, central sections of the pile are respectively 608 kNm, 757 kNm, 206 kNm and 233 kNm (after Berrill et al., 2001). They also estimated the passive force coming from the non-liquefied crust to be around 850 to 1000 kN per pier and the drag force from the liquefied soil to be 50 kN from a set of 8 piles. As the collapse load of the pier system is 1207 kN, failure did not occur.

Berrill et al (2001) concludes that,

"*The chief threat to piled foundations from lateral spreading comes from loads imposed by the non-liquefiable crust, not from the drag forces of the liquefied soil*".

They also conclude that, "*the full collapse mechanism had not developed since the piers were still very near vertical*". From the point of view of this study it is interesting point to note that the piles passed through 4 m of liquefiable soil and the section of the pile is 406 mm square. The piles were raked and hence the boundary condition of the pile may be assumed as fixed-fixed condition.

Case history 3

14 storey building during the Kobe Earthquake of January 17, 1995

The third case study relates to the good performance of a 14-story building on piled foundation near American park in a laterally spreading soil (Tokimatsu et al., 1996). American park is a place in Chuo-Ku that faces the port of Kobe. On the pier at the park, this 14-storey building was under construction when the earthquake took place. The building was supported on cast-in place concrete piles 2.5 m in diameter and 33 metres long. The piles passed through 12.2m in liquefiable soil. During the earthquake, the quay wall on the west, south, and east of the building moved horizontally by 1 m, 2 m and 0.5-0.6 m and settled by 0.4-0.6 m, 0.5-0.7 m and 0.2-0.3 m respectively. Figure 3.11 shows the section and plan of the building.

Tokimatsu et al (1996) reports that the building survived without damage to its pile foundation probably due to the deep cement mixing (DCM) walls that surrounded the piles.

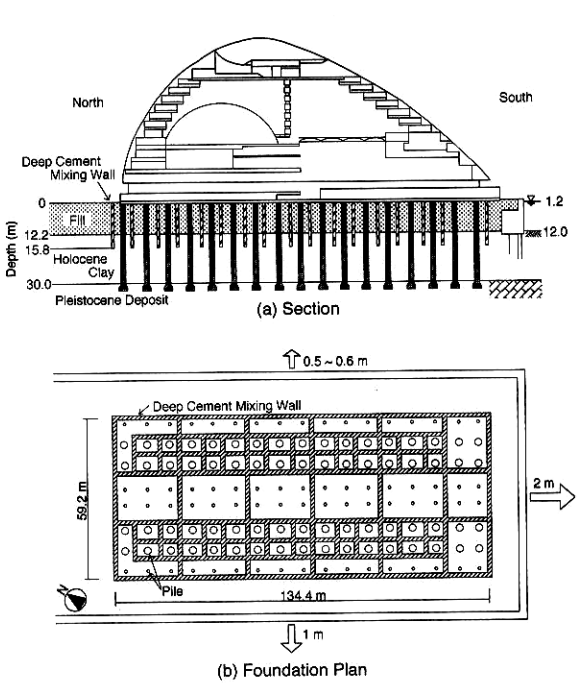

Figure 3.11: Section and plan of a building founded on piles surrounded by deep cement mixing walls (after Tokimatsu et al., 1996).

Case history 4

Kobe Shimim Hospital during the 1995 Kobe earthquake

The fourth case study presents the good performance of a hospital building during the 1995 Kobe earthquake. The hospital is located in the interior of the Port Island and the depth of liquefiable fill is approximately 16 to 18 m (Soga, 1997). The hospital remained in place and the surrounding ground subsided. The hospital had a basement extending 9.8m below the foundation. The piles are steel piles having a diameter of 0.66 m and length of 30.15 m. The piles pass through 6.2 m in liquefiable soil. Figure 3.12 shows the section of the hospital along with the soil profile.

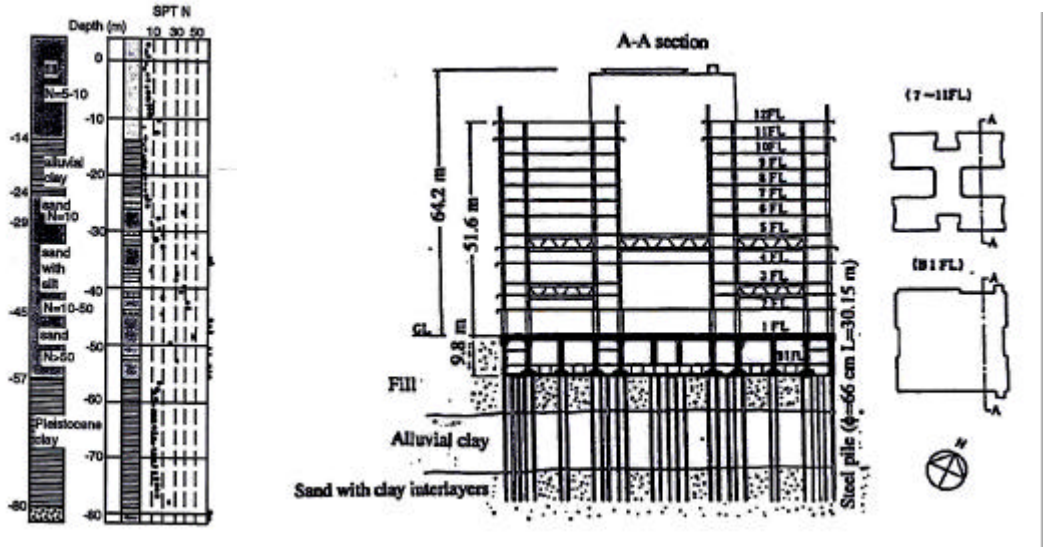

Figure 3.12: Figure showing the section of the Kobe Shimim hospital along with the soil profile, Soga (1997).

Case history 5

Hanshin Expressway during the 1995 Kobe earthquake

This is the case history of the good performance of the substructure of Hanshin Expressway during the 1995 Kobe earthquake. It has been reported by Ishihara (1997) that little damage was incurred to the piles. The piles pass through 15 m in liquefiable soil and have a diameter of 1.5 m. The pile cap is 22.5 m long by 14.5 m wide and contains 22 piles as shown in Figure 3.13. The boundary condition of the pile can be described as shown in Figure 3.6. Figure 3.13 also shows the soil profile in the expressway site.

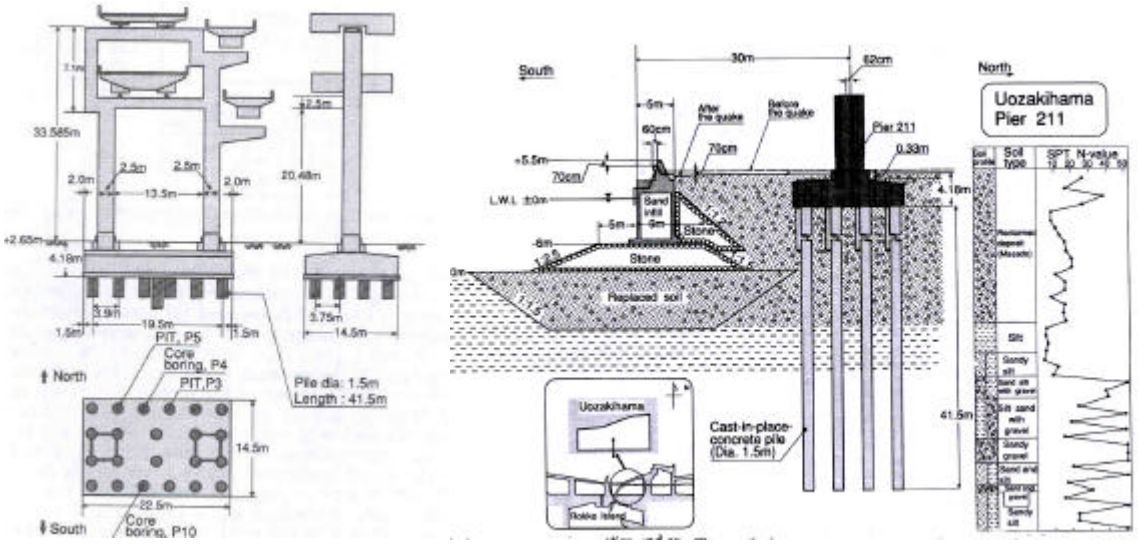

Figure 3.13: (a) Figure showing the superstructure of the expressway along with the cross section of the piles. The figure also shows the pile-cap, Ishihara (1997); (b): Figure showing the soil profile of the Hanshin expressway along with the piles, Ishihara (1997).

Case history 6

LPG Tank 101 during the 1995 Kobe earthquake

The sixth case study shows the good performance of Liquefied Propane Gas (LPG) tanks in the man made islands in the port area of Kobe. Tank no 101 suffered practically no damage. The foundation of tank 101 consists of 97 cast-in-placed reinforced concrete piles. The arrangement of the piles in plan and section is shown in the Figure 3.14 along with the soil profile. Each pile has a diameter of 1.1 m and is embedded to a depth of 27 meters. From the soil profile it is most likely that the top 15 m rests in liquefiable soil. During the earthquake the tank contained 6700kL of LPG. The boundary conditions of the pile are shown in Figure 3.4.

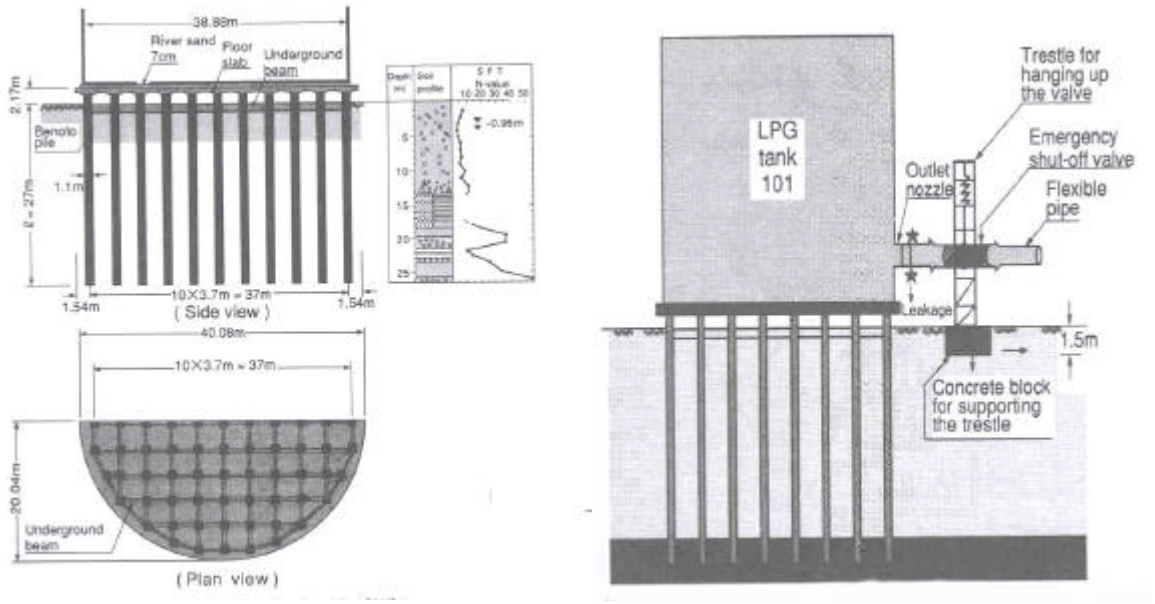

Figure 3.14: Figure showing the plan elevation and section of the tank 101 along with the soil profile along the length of the pile.

3.3.2 Poor performance of pile foundations

Table 3.3 lists the shows the case histories reported in this section along with the reference of the authors.

Table-3.3: Poor performance of pile foundation analysed.

Index no	Earthquake	Structure type	Reference
7	1964 Niigata earthquake, Japan	NHK building	Hamada (1992a)
8	1964 Niigata earthquake, Japan	NFCH building	Hamada (1992a)
9	1964 Niigata earthquake, Japan	Showa bridge over river Shinano	Hamada (1992a)
10	1964 Niigata earthquake, Japan	Yachiyo Bridge abutment	Hamada (1992a)
11	1983 Chubu earthquake, Japan	Gaiko Ware House	Hamada (1992b)
12	1995 Kobe earthquake	4 storey fire house	Tokimatsu et al., (1996)
13	1995 Kobe earthquake	3 storied building at Kobe University.	Tokimatsu et al., (1996)
14	1995 Kobe earthquake	Elevated port liner railway	Soga (1997)
15	1995 Kobe earthquake	LPG tank 106, 108	Ishihara (1997)

This section describes the case histories along with the reported damage features. The parameters of the analysis are mentioned in Table 3.4. Detailed calculations of the parameters of Yachiyo Bridge pile foundation (case history 10) is shown in Appendix-C.

Case History 7

NHK building during the 1964 Niigata earthquake

The seventh case study illustrates the failure of piles in the N.H.K building. This is a four-storey R.C building supported on reinforced concrete piles. The piles have a diameter of 350 mm solid section and are 11 to 12 m long. After the earthquake, 74 piles were investigated (see Figure 1.3b) and it was found that all of them were similarly damaged (see Hamada, 1992a). The piles failed at two positions, 2.5 to 3.5 m from the upper end of the piles and 2.0 to 3.0m from the bottom as shown in Figure 3.15. The liquefied layer was estimated to be around 10m and thus the pile was founded 1m to 2 m in non-liquefiable layer.

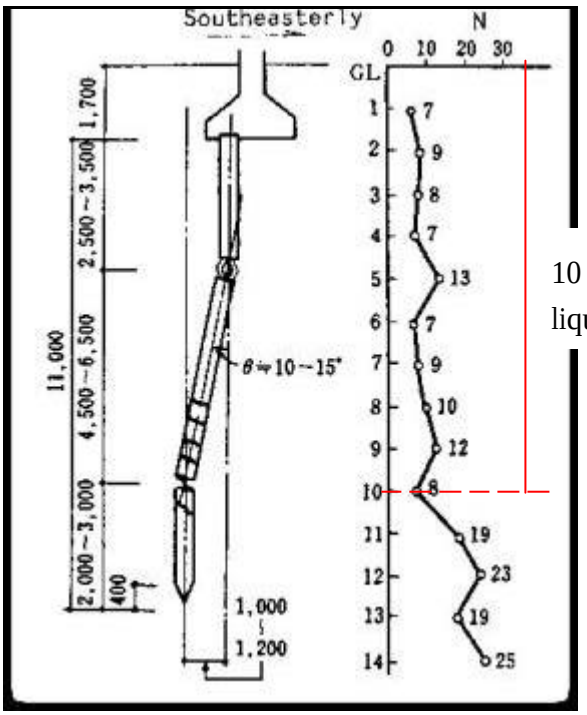

Figure 3.15: Failed piles of N.H.K building (after Hamada, 1992a).

From Figure 3.15 it may be noted that the pile base rotated 10 to 15 degrees and this suggests that pile base was pinned. Following Figure 3.2(c) the effective length of the pile is twice the length of the pile in liquefiable soil. The table below quotes the parameters.

L_{eff} of the pile in liquefiable zone	**r_{min} of the pile**	**Slenderness ratio**	**Conventionally Allowable load**	**Buckling load of the pile**
20m	0.09m	222	430kN	450kN

Thus, it can be seen that during liquefaction, the pile had a load very near to Euler's critical load

Case history 8

Niigata Family Court House (NFCH) building

This case study describes the failure of a four-storey R.C building constructed on hollow concrete piles. The pile had a diameter of 350 mm and thickness of 75 mm. After the earthquake the building tilted about 1degree. Figure 1.3(a) shows the structural arrangement of the building. The pile only extended 500mm in the non-liquefied layer and can be assumed as pinned bottom. The photograph of Figure 3.16 corresponds to failure of Pile 2 in Figure 1.3(a).

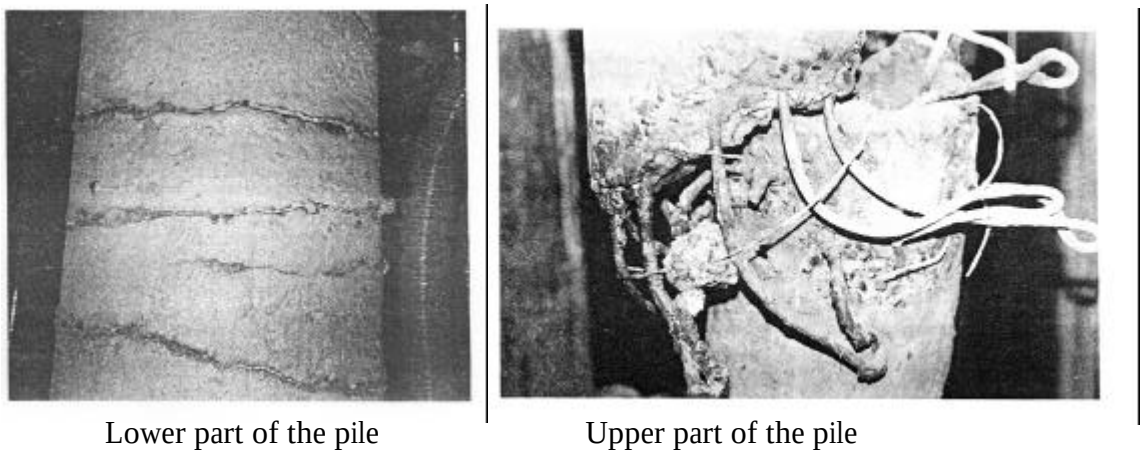

Lower part of the pile Upper part of the pile

Figure 3.16: Failure of pile marked 2 of Niigata family Court House (after Hamada, 1992a).

The table below quotes the parameters in the analysis.

L_{eff} of the pile in liquefiable zone	**r_{min} of the pile**	**Slenderness ratio**	**Conventionally Allowable load**	**Buckling load of the pile**
16m	0.1m	160	287kN	630kN

This case history is widely used as benchmark problem for numerical analysis and the applied load quoted is 292 kN, such as O' Rourke et al. (1994). The shear capacity is estimated to be 19.5 kN.

Case History 9

Failure of Showa Bridge over river Shinano during the 1964 Niigata earthquake

Figures 1.2(b), 1.7, 1.8 and 3.3(a) show the failure of the 10-span 307 m long Showa Bridge. Section 3.2.1 describes the superstructure of the bridge and also estimates the allowable load on the pile. From Figure 3.3 it may be noted that the pile passes through 10 m of potentially liquefiable soil and is founded on 6 m of competent non-liquefiable soil. The length of the pile in liquefiable zone is 10m and the length of pile in free air / water is 9 m.

Thus the pile length in unsupported zone during liquefaction is 19 m. From the buckled shape (shown as original position in Figure 3.3 (a)), it is clear that the pile had fixed-free boundary conditions and hence the effective length is twice the length in unsupported zone. It is also in some way similar to the shape observed in Figure 3.1. The following section estimates the buckling load of the pile.

STRUCTURAL PROPERTIES OF PILE

Moment of inertia of the pile (I) $= \frac{p}{64}\left(0.609^4 - 0.591^4\right)m^4 = 7.63\times10^{-4}m^4$

Effective length of pile (L_{eff}) = 2 × 19m = 38m

BUCKLING LOAD OF PILE $= \frac{p^2}{L_{eff}^2}EI = \frac{p^2}{38^2\,m^2}\times 210GPa\times 7.63\times10^{-4}m^4 = 1095kN$

Structural engineers generally demand a load factor of at least 2 against linear elastic buckling to allow for eccentricities and reduction of stiffness due to yielding.

L_{eff} of the pile in liquefiable zone	**r_{min} of the pile**	**Slenderness ratio**	**Conventionally Allowable load**	**Buckling load of the pile**
38m	0.21m	181	965kN	1095kN

Case history 10

Failure of the Yachiyo Bridge over river Shinano during the 1964 Niigata earthquake

The tenth case study presents the damage of Yachiyo Bridge over river Shinano adjacent to Showa Bridge. Extensive lateral spreading occurred in the river and the river width decreased. Figure 3.17 illustrates the damage to the abutments and piers of the bridge. The foundations of both abutments and piers were RCC piles of 300 mm in diameters and a length of 10 to 11 m. The figure also shows the deformed shape after excavation. The pile can be seen to form a plastic hinge at the depth of 8 m i.e. at the bottom of the liquefiable layer. The pile head displaced by 1.1m whereas the free field deformation is reported to be 2 to 5 metres, (see Dobry and Abdoun, 2001).

The buckling load is estimated to be 383kN whereas the allowable load is 340kN. Appendix C shows in detail derivation of these parameters.

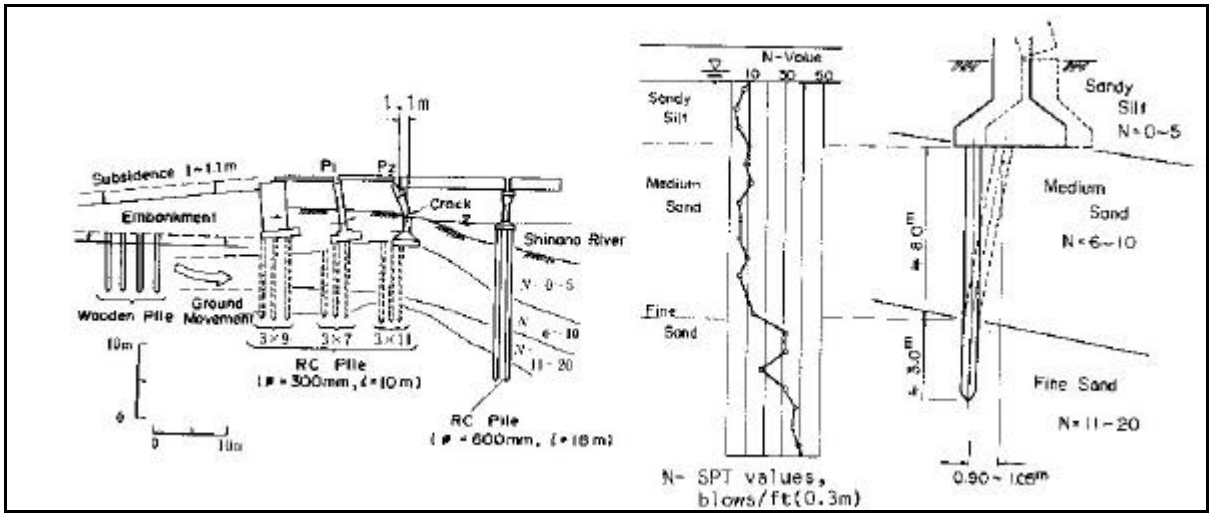

Figure 3.17: Failure of Yachiyo Bridge after Hamada (1992a).

Case history 11

Gaiko Ware house during the 1983 Chubu earthquake

This case study depicts the damage of the Gaiko Landing warehouse during the 1983 Chubu earthquake. The warehouse was founded on prestressed concrete piles, 600mm outer diameter, 100 mm thick and 18 m long. After the earthquake the ground was excavated and the pile damage was studied using inclinometers (see Hamada, 1992b). From the damage survey of the pile (Figure 3.18), it is noted that it is likely that piles were damaged at the levels of 7.5 m and around 15 m. Details can be seen in Hamada (1992b). From the soil investigation report the depth of liquefiable layer is estimated to be around 14 m.

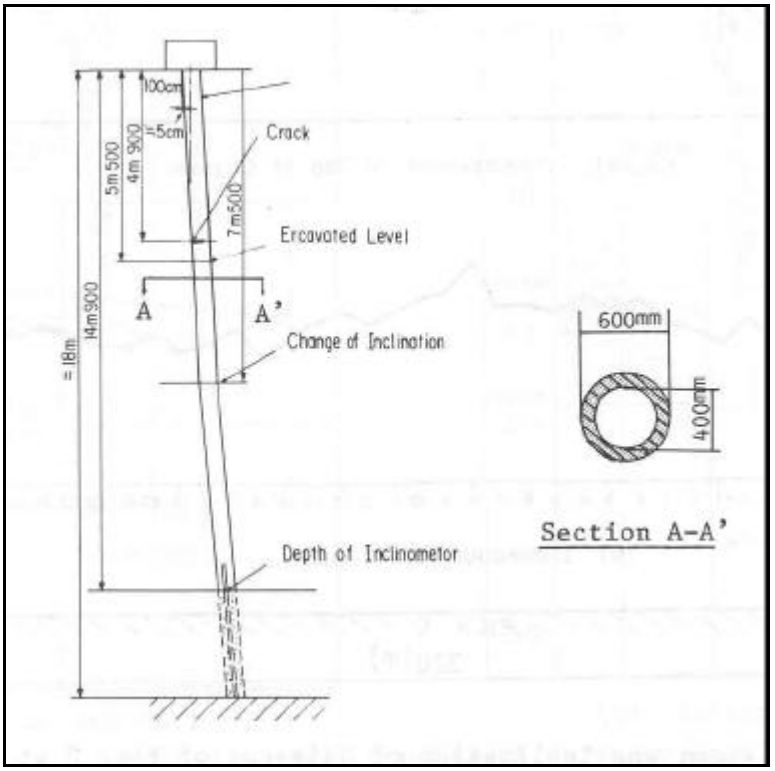

Figure 3.18: Damaged piles in Gaiko warehouse after 1983 Chubu earthquake after Hamada (1992b).

Case history 12

Failure of 4-storey firehouse during the 1995 Kobe earthquake

This case study is the failure of a four-storied firehouse building at the foot of the Kobe O-Hashi Bridge on Port Island. The building moved and tilted towards the sea. The foundation of the building consisted of 400 mm diameter prestressed concrete piles 30 m long, Tokimatsu et al. (1996). Post earthquake excavation survey showed that compressional shear failure occurred on the seaside with minor flexural cracks on the opposite side. From the soil report of Port Island, it is estimated that the top 18 m is most likely to have liquefied during the earthquake.

Case history 13

Poor performance of a three storied building at Fukae during the 1995 Kobe earthquake

The pile-supported building was constructed in early 1980's on reclaimed land. The section and foundation plan of the building are shown in Figure 3.19(a). The piles were 400 mm diameters and 20 m long. Extensive soil liquefaction as well as lateral spreading was observed at the building site, Figure 3.19(b). After the earthquake, the building tilted by 3 degrees towards the sea without any structural damage of the superstructure. Comparing the aerial photograph before and after the earthquake, the displacement of the pile head is estimated to be around 800 mm, Tokimatsu et al. (1998). From the boring log data of the site before construction, it is estimated that the top 16m of the pile is in liquefiable soil.

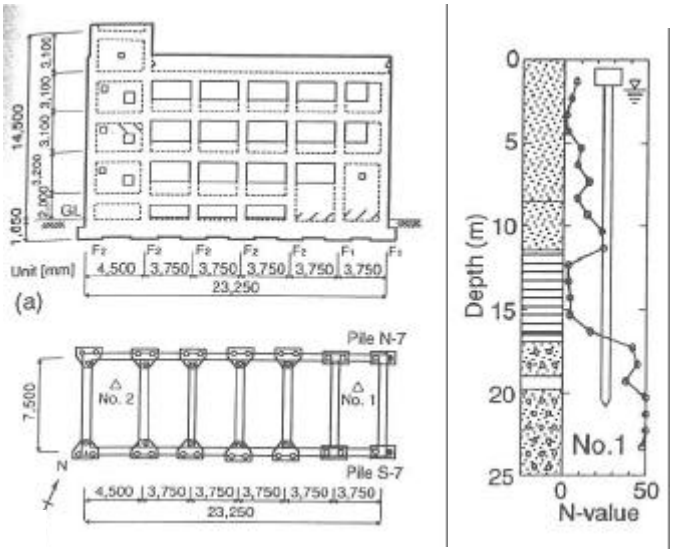

Figure 3.19(a): Plan and section of the building along with the bore log data of the pile.

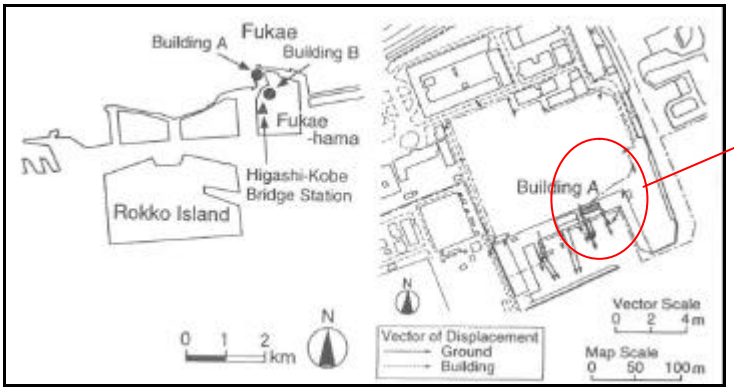

Figure 3.19(b): Location of the building.

Case history 14

Elevated port liner railway

Some of the pile supported piers of the elevated port liner railways on Port Island were damaged. Each pier was supported by 600 mm RCC piles. Cracks were reported to be found in the piles during the excavation of the surrounding ground, Soga (1997). The piles were 32.5 m long and passed 12 m through the liquefiable soil.

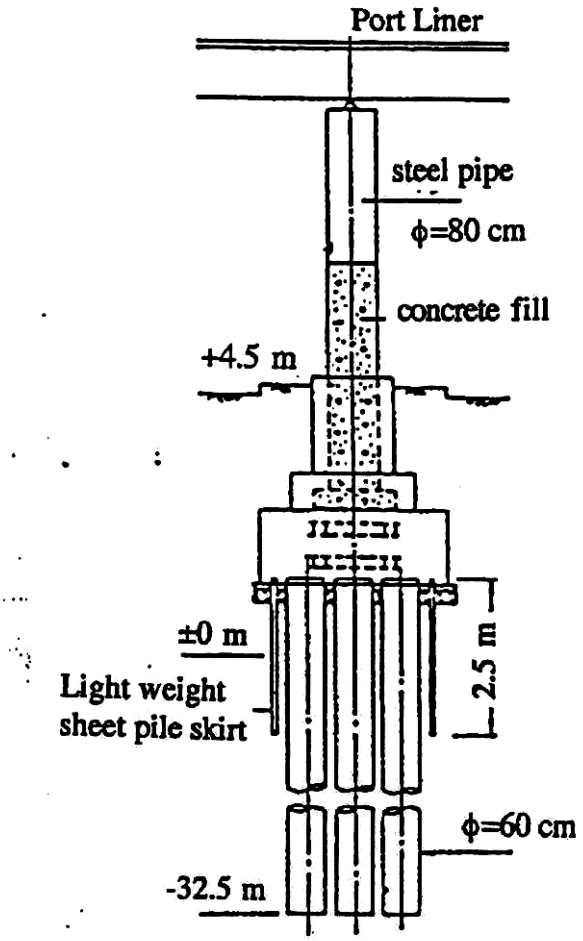

Figure 3.20: Foundation of the port liner railway, after Watanabe (1981)

Case history 15

Poor performance of the LPG tanks 106, 107 during the 1995 Kobe earthquake

These tanks were located at the same site where tank 101 was located (Case history 6), Figure 3.21(a). Figure 3.21(b) shows the details of the pile foundation supporting the tank. The piles had a diameter of 300mm and 20m long. Post earthquake survey revealed that the tank tilted by 3.6% and also showed a differential settlement of the order of 270mm (see Ishihara, 1997). The integrity of the piles were tested using borehole video camera. Results of the survey showed that cracks in the piles developed mostly between 5m and 10m. The depth of the liquefiable layer at this site is 15m (see Figure 3.4, Case history 6).

(a) (b)

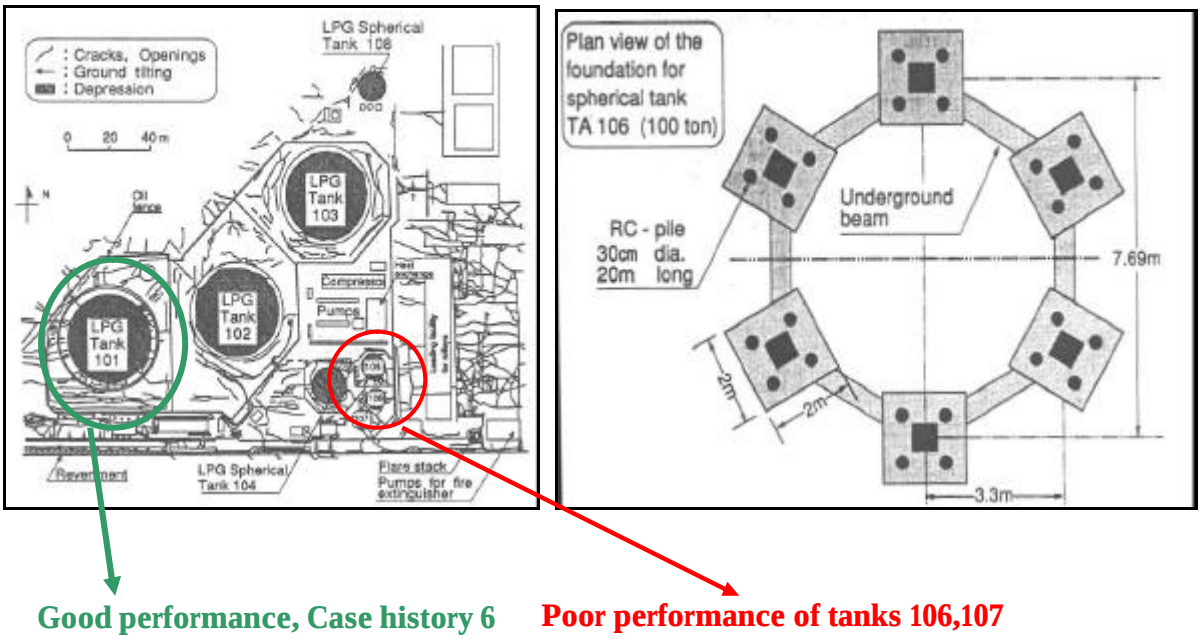

Figure 3.21: LPG tanks after Ishihara (1997); (a): Locations of the tanks; (b): Foundation arrangement of tanks 106 and 107.

Table 3.4: Summary of pile performances

Sl no.	Case History and Reference.	L* (m)	L_0** (m)	Pile section/ type	Framing action/b*** value	L_{eff} (m)	r_{min} (m)	L_{eff}/r_{min}	P MN	P_{cr} MN	s MPa	Lateral spreading observed?	Performance
1	10 storey-Hokuriku building, 1964 Niigata earthquake, Hamada (1992)	12	5	0.4m dia RCC	Large piled raft with basement. 1	5.0	0.1	50	0.77	12.4	6.2	Yes, nearby ground moved by 2m.	Good
2	Landing bridge, 1987 Edgecumbe earthquake, Berrill et al (2001)	9	4	0.4m square PSC	Raked piles, no sway frame 0.5	2.0	0.12	17	0.62	139	3.8	Yes, ground cracked and sand ejected.	Good
3	14 storey building in American park, 1995 Kobe earthquake, Tokimatsu et al (1996)	33	12.2	2.5m dia RCC	Large pile group and large pile dia. 1.0	12.2	0.63	19	19	3183	3.8	Yes, quay walls on the west, south and east moved.	Good
4	Kobe Shimim hospital, 1995 Kobe earthquake, Soga (1997)	30	6.2	0.66m dia Steel tube	Large piled raft with basement. 1.0	6.2	0.23	27	3.0	91	92.6	No, Ground subsided.	Good
5	Hanshin expressway pier, 1995 Kobe earthquake, Ishihara (1997)	41	15	1.5m dia RCC	Small group (22 piles) 1.0	15	0.38	40	14	272	7.9	Yes, ground moved by 0.62m.	Good
6	LPG tank 101, Kobe earthquake, Ishihara (1997)	27	15	1.1m dia RCC	Large piled raft 1.0	15	0.28	53	4.1	79	4.3	Yes, ground moved by 0.7m.	Good
7	N.H.K building, 1964 Niigata earthquake, Hamada (1992)	12	10	0.35m dia RCC	Groups tied by flexible beam, Less embedment at pile tip. 2.0	20	0.09	222	0.43	0.45	4.4	Yes, nearby ground moved by 2m.	Poor

Sl no.	Case History and Reference.	L* (m)	L_0** (m)	Pile section / type	Framing action / b*** value	L_{eff} (m)	r_{min} (m)	L_{eff}/r_{min}	P MN	P_{cr} MN	s MPa	Lateral spreading observed?	Performance
8	NFCH building, 1964 Niigata earthquake, Hamada (1992)	9	8	0.35m dia RCC hollow	Groups tied by flexible beam, Less embedment at pile tip 2.0	16	0.10	160	0.29	0.63	4.5	Yes, nearby ground moved by 1 to 2m.	Poor
9	Showa bridge, 1964 Niigata earthquake, Hamada (1992)	25	19	0.6m dia Steel tube	A single row of piles 2.0	38	0.21	181	0.96	1.10	56.3	Yes, width of river decreased.	Poor
10	Yachiyo Bridge, 1964 Niigata earthquake, Hamada (1992)	11	8	0.3m dia RCC	Isolated footing 2.0	16	0.08	200	0.34	0.39	4.8	Yes, width of river decreased.	Poor
11	Gaiko Ware House, 1983 Chubu earthquake, Hamada (1992)	18	14	0.6m dia PSC hollow	Isolated footing 2.0	28	0.16	175	1.47	1.61	9.3	Yes, nearby ground moved by 1.5m.	Poor
12	4 storey fire house, 1995 Kobe earthquake, Tokimatsu et al (1996)	30	18	0.4m dia PSC	Groups tied by beam. 1.0	18	0.10	180	0.89	0.96	7.0	Yes, building moved and tilted towards the sea.	Poor
13	3 storied building at Fukae, 1995 Kobe earthquake, Tokimatsu et al (1998)	20	16	0.4m dia PSC hollow	Groups tied by beam. 1.0	16	0.12	133	0.72	1.02	9.4	Yes, building moved and tilted towards the sea.	Poor
14	Elevated port liner railway, 1995 Kobe earthquake, Soga (1997)	30	12	0.6m dia RCC	Isolated footing, large embedment at pile tip. 1.0	12	0.15	80	1.38	10.92	4.9	Yes,	Poor, cracks were seen in some of the piles.

Sl no.	Case History and Reference.	L* (m)	L_0** (m)	Pile section / type	Framing action / b*** value	L_{eff} (m)	r_{min} (m)	L_{eff}/r_{min}	P MN	P_{cr} MN	s MPa	Lateral spreading observed?	Performance
15	LPG tank 106,107 –1995 Kobe earthquake, Ishihara (1997)	20	15	0.3m dia RCC hollow	Groups tied by beams. 1.0	15	0.08	187	0.46	0.38	6.6	No, ground subsided.	Poor

* L = Length of the pile;

** L_0 = Length of pile in liquefiable region / buckling zone.

*** β = Factor for estimating effective length. $L_{eff} = \beta L_0$.

3.4 Analysis and Discussion

The case histories reported in the earlier section are collated to form Table 3.4. Figure 3.24 shows the effective length of the piles in a liquefiable zone plotted against the r_{min} of the pile section. A line representing a slenderness ratio (L_{eff}/r_{min}) of 50 is shown. The line distinguishes piles of poor performance from the piles of good performance. This line is of some significance in structural engineering, as it is often used to distinguish between "long" and "short" columns. Columns having slenderness ratios below 50 are expected to fail in crushing whereas those above 50 are expected to fail in buckling instability.

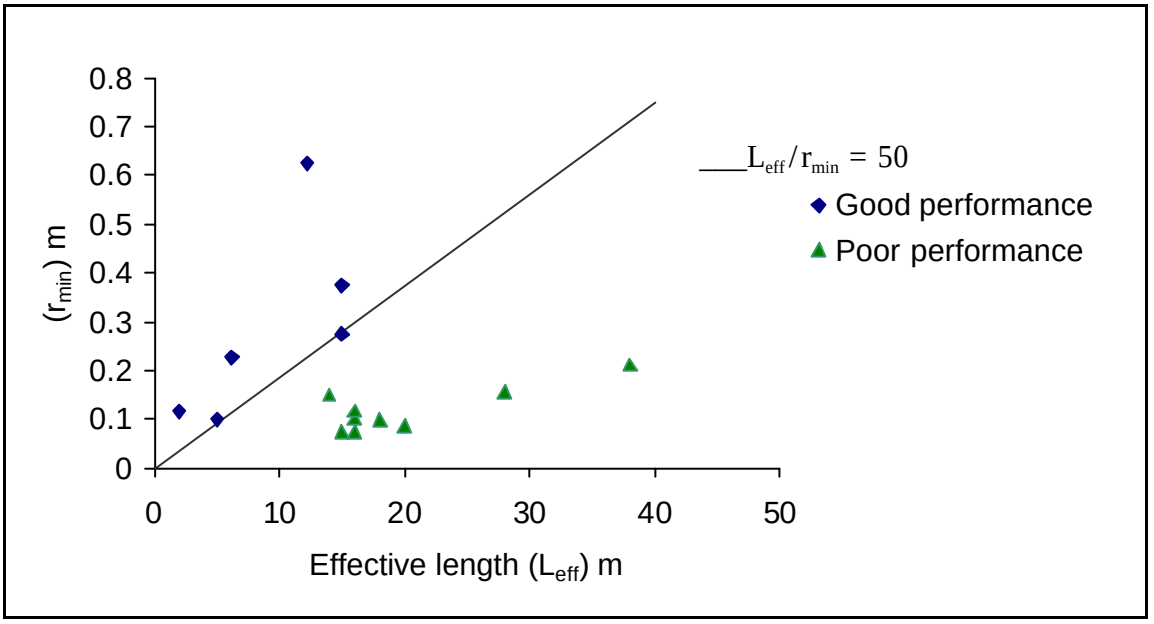

Figure 3.24: L_{eff} versus r_{min} for piles studied

Figure 3.25 shows the plot of 13 concrete piles mentioned in Table 3.4. The piles are assumed to be of M25 grade concrete (BS 8110), with a characteristic strength of 25 MPa. In the plot, three well-defined lines are drawn. These are:

1. Yield stress line (σ_y = 11.2 MPa) taken as the design crushing value,
2. Euler's curve for σ_{cr}, given by equation 3.3 which is the elastic stability limit obtained by substituting the value of I from equation 2.1 into equation 3.1 and noting that σ_{cr} is the critical stress given by (P_{cr}/A)

$$s_{cr} = \frac{P_{cr}}{A} = \frac{p^2}{\left(\frac{L_{eff}}{r_{min}}\right)^2} E \qquad (3.3)$$

3. A curve for σ_f drawn using Rankine's formula (1866) shown by equation 3.4. This design curve mediates the transition between strength and stability. Many other similar curves, such as Perry-Robertson (1886 & 1925), can equally be used.

$$\frac{1}{s_f} = \frac{1}{s_{cr}} + \frac{1}{s_y} \qquad (3.4), \text{ where}$$

σ_y is yield stress of the material and σ_{cr} is the elastic critical stress as calculated by equation 3.3, leading to an estimate of the combined failure stress σ_f.

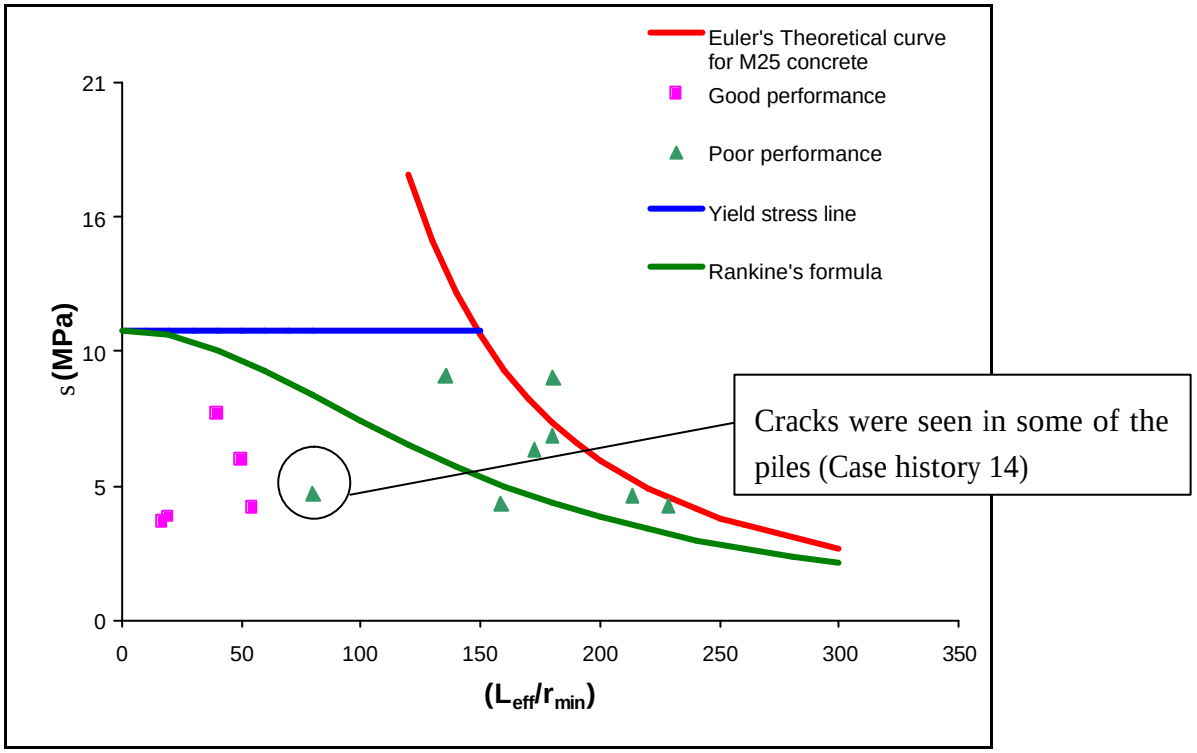

Figure 3.25: Plot of concrete pile performance mentioned in Table 3.4.

Figure 3.26 plots the allowable load (P) against the Euler's buckling load (P_{cr}) for the piles that failed. It may be observed that the piles that failed had P/P_{cr} ratio between 0.5 and 1. On the other hand, from Table 3.4, it may be noted that the piles that survived the earthquake had (P/P_{cr}) ratio below 0.1.

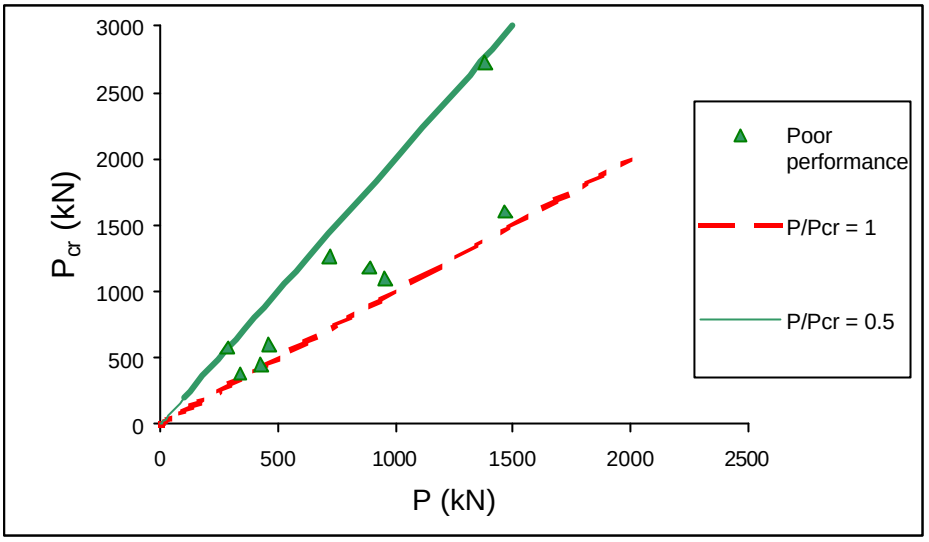

Figure 3.26: Plot of the poor performance of piled foundations.

The study of the case histories seems to show a dependence of pile performance on buckling parameters. As short columns fail in crushing and long columns in buckling, the analysis suggests that pile failure in liquefied soils is similar in some ways to the failure of long columns in air. The lateral support offered to the pile by the soil prior to the earthquake is removed during liquefaction. This hypothesis is shown in Figure 3.27 and explained in section 3.5.

3.5 Hypothesis arising from the study of case histories

During earthquakes, soil layers overlying the bedrock are subjected to seismic excitation consisting of numerous incident waves, namely shear (S) waves, dilatational or pressure (P) waves, and surface (Rayleigh and Love) waves which result in ground motion. The ground motion at a site will depend on the stiffness characteristics of the layers of soil overlying the bedrock. This motion will also affect a piled structure. As the seismic waves arrive in the soil surrounding the pile, the soil layers will tend to deform. This seismically deforming soil will try to move the piles and the embedded pile-cap with it. Subsequently, depending upon the rigidity of the superstructure and the pile-cap, the superstructure may also move with the foundation. The pile may thus experience two distinct phases of initial soil-structure interaction.

1) Before the superstructure starts oscillating, the piles may be forced to follow the soil motion, depending on the flexural rigidity (EI) of the pile. Here the soil and pile may

take part in kinematic interplay and the motion of the pile may differ substantially from the free field motion. This may induce bending moments in the pile.

2) As the superstructure starts to oscillate, inertial forces are generated. These inertia forces are transferred as lateral forces and overturning moments to the pile via the pile-cap. The pile-cap transfers the moments as varying axial loads and bending moments in the piles. Thus the piles may experience additional axial and lateral loads, which cause additional bending moments in the pile.

These two effects occur with only a small time lag. If the section of the pile is inadequate, bending failure may occur in the pile. The behaviour of the pile at this stage may be approximately described as a beam on an elastic foundation, where the soil provides sufficient lateral restraint. The available confining pressure around the pile is not expected to decrease substantially in these initial phases. The response to changes in axial load in the pile would not be severe either, as shaft resistance continues to act. This is shown in Figure 3.27 (b).

In loose saturated sandy soil, as the shaking continues, pore pressure will build up and the soil will start to liquefy. With the onset of liquefaction, an end-bearing pile passing through liquefiable soil will experience distinct changes in its stress state.

- The pile will start to lose its shaft resistance in the liquefied layer and shed axial loads downwards to mobilise additional base resistance. If the base capacity is exceeded, settlement failure will occur.
- The liquefied soil will begin to lose its stiffness so that the pile acts as an unsupported column as shown in Figure 3.20(c). Piles that have a high slenderness ratio will then be prone to axial instability, and buckling failure may occur in the pile, enhanced by the actions of lateral disturbing forces and also by the deterioration of bending stiffness due to the onset of plastic yielding.

In sloping ground, even if the pile survives the above load conditions, it may experience additional drag load due to the lateral spreading of soil. Under these conditions, the pile may behave as a beam-column (column with lateral loads); see Figure 3.27(d).

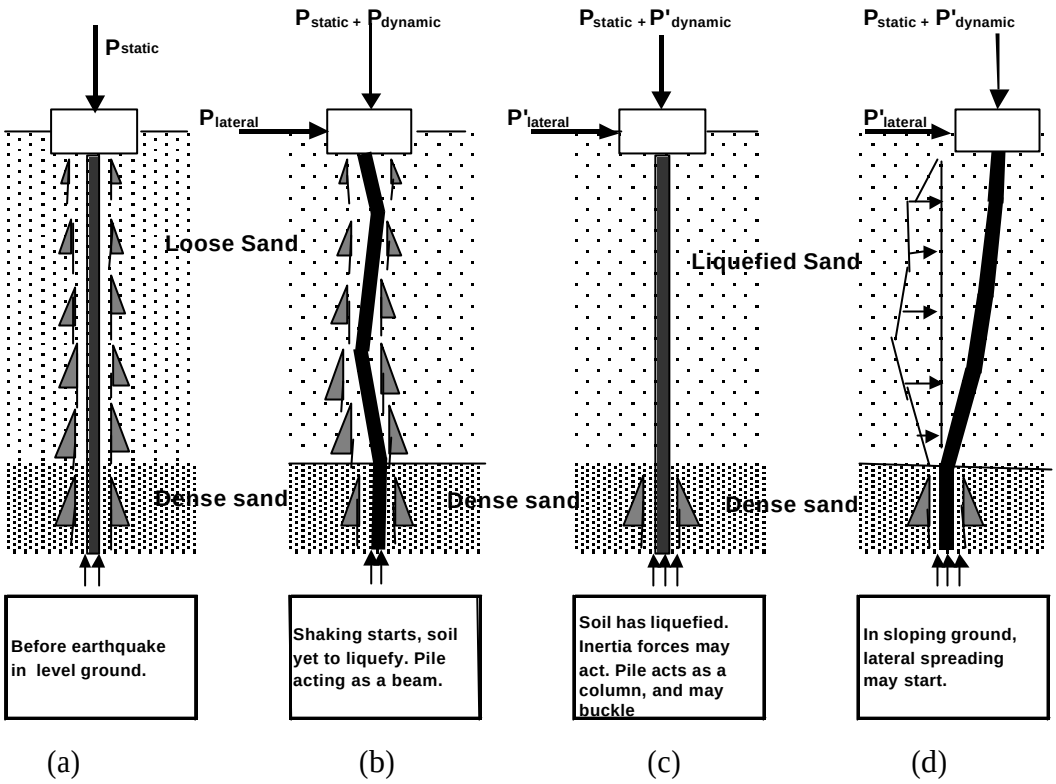

Figure 3.27: The time history of loading in the proposed failure mechanism**.**

3.6 Summary

Fifteen cases of pile foundation performance have been analysed. The study of case histories hints that buckling may be a possible failure mechanism. However, there are many uncertainties involved in the parameters used to study the case histories. The parameter r_{min} has no uncertainty. Other parameters, for example, L_{eff} and P_{cr} depend on the correct estimation of the depth of liquefiable soil. P, the actual load acting on the pile can be quite different from the allowable load of the pile obtained from conventional procedure.

While it appears that buckling is a possibility, it must also be expected that when the pile tends to buckle sideways it has to shear the soil in front of it. This shearing would dilate the soil in the sheared zone, which would generate suctions and may stiffen the soil-pile system and buckling may not be an issue (see Haigh, 2002). One of the ways to verify the buckling mechanism is through controlled physical modelling such as dynamic centrifuge tests.